

## 5 Meson Spectroscopy at LEAR with the Crystal Barrel

C. Amsler, P. Giarritta, M. Heinzemann and C. Regenfus

*in collaboration with:*

Academy of Science (Budapest); Universities of Bochum, Bonn, Hamburg, Karlsruhe, München, Paris VI; CERN; Carnegie Mellon University (Pittsburgh); CRN (Strasbourg); RAL; UC (Berkeley)

(CRYSTAL BARREL COLLABORATION)

During 1999 we finalized the analysis of proton-antiproton annihilation at rest into  $\omega\pi^0\pi^0$  and  $\omega\eta\pi^0$  ( $7\gamma$  final state) and antiproton-deuteron annihilation into  $\Lambda K^0$  and  $\Sigma^0 K^0$ . The analysis of proton-antiproton annihilation in flight into three neutral pseudoscalar mesons at 900 MeV/c ( $6\gamma$  final state) also nears completion. We shall first briefly summarize the final conclusions on the  $7\gamma$  and our progresses in the  $6\gamma$  final states. Preliminary results were presented in last year's annual report. We then discuss our analysis of antiproton-deuteron annihilation in somewhat more details.

### 5.1 Proton-antiproton annihilation into $6\gamma$ and $7\gamma$

The annihilation channels  $\bar{p}p \rightarrow \omega\eta\pi^0$  and  $\omega\pi^0\pi^0$  at rest, leading to 7 detected  $\gamma$ 's ( $\eta, \pi^0 \rightarrow \gamma\gamma$  and  $\omega \rightarrow \pi^0\gamma$ ), were analyzed with the full available data samples, giving 34,064 and 136,023 events, respectively, and taking into account the angular distribution of the  $\gamma$  in the  $\omega$  rest frame [1]. The data were analyzed with the K-matrix formalism which fulfils unitarity for broad overlapping resonances and describes two or more open channels competing in resonance decays. In contrast to earlier work [2] using the Breit-Wigner formalism, a completely satisfactory description of the channel  $\omega\pi^0\pi^0$  is now achieved, with contributions from  $b_1(1235)\pi^0$ ,  $\omega f_2(1270)$  and  $\omega(\pi\pi)_S$ , where  $(\pi\pi)_S$  is the  $\pi\pi$  S-wave that was studied earlier in great details by our collaboration [3].

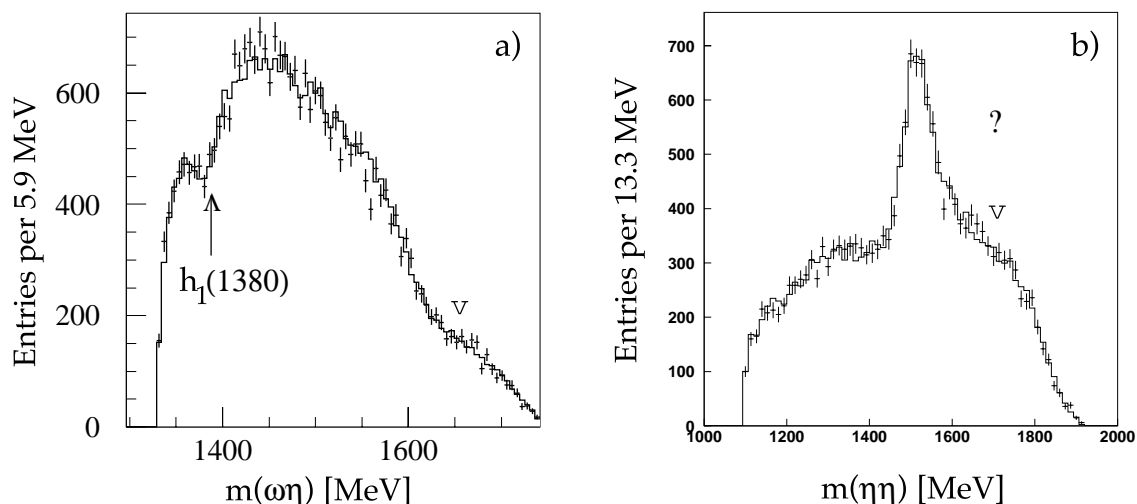


Figure 5.1: a)  $\omega\eta$  mass distribution in  $\bar{p}p \rightarrow \omega\eta\pi^0$  at rest. The dip at 1380 MeV is due to a  $1^{+-}$  state decaying to  $\omega\eta$  near the  $K^*\bar{K}$  threshold. The enhancement at 1700 MeV (arrow) is due to a  $1^{--}$  (vector) meson. The histogram shows the K-matrix fit; b)  $\eta\eta$  mass distribution in  $\eta\eta\pi^0$  at 900 MeV/c. The peak is due to  $f_0(1500)/f'_2(1525)$ . There is no evidence for  $f_0(1710)$  (arrow). The shoulder around 1750 MeV is due to a reflection of  $a_0(980) \rightarrow \eta\pi$ .

From the channel  $\omega\eta\pi^0$  we obtain evidence for two mesons decaying to  $\omega\eta$ . The present data are the first observations of mesons decaying to  $\omega\eta$ . A  $1^{+-}$  isoscalar meson is observed at a mass of  $1382 \pm 2$  MeV, with a width of  $65 \pm 14$  MeV. The dip in the distribution (fig.5.1a) is due to the competing decay channel  $K^*\bar{K}$  which opens at this mass. It is identified as the  $h_1(1380)$ , the isospin zero partner of  $h_1(1170)$ , in which case we determine a singlet-octet mixing angle of  $-5.4_{-1.6}^{+2.7^\circ}$  in the  $J^{PC} = 1^{+-} q\bar{q}$  nonet. The  $h_1(1380)$  was so far poorly established. A weak signal at this mass was reported earlier, albeit in  $K^*\bar{K}$  [4, 5]. At 1698 MeV one observes a 111 MeV broad  $1^{--}$  meson (fig.5.1a). Two vector mesons were reported earlier around this mass,  $\omega(1600)$  and  $\phi(1680)$ , decaying to  $\rho\pi\pi$  and  $\omega\pi$ .

The  $f_0(1710) \rightarrow \eta\eta$  meson was searched for in  $\bar{p}p$  annihilation in flight into  $\eta\eta\pi^0$  ( $6\gamma$  final state) at 900 MeV/c [6, 7]. The spin of  $f_0(1710)$  was recently established in  $pp$  central collisions to be zero. The data from central collisions at 450 GeV point to a dominant  $s\bar{s}$  structure and therefore provide a strong evidence for the so far missing  $s\bar{s}$  member of the scalar nonet. On the other hand, the  $f_0(1500)$  is also observed in central collisions, but not in  $\gamma\gamma$ . This and the  $s\bar{s}$  structure of  $f_0(1710)$  add supportive evidence for the glueball nature of  $f_0(1500)$  [8]. If  $f_0(1710)$  were pure  $s\bar{s}$  it should not be produced from the  $\bar{p}p$  system which does not contain any  $s$ -quark. Figure 5.1b shows the  $\eta\eta\pi^0$  mass projection with, indeed, no striking evidence for a state around 1700 MeV. However, the amplitude analysis requires a 300 MeV broad  $2^{++}$  state around 1900 MeV [6]. The analysis of the  $3\pi^0$  and  $2\pi^0\eta$  channels at 900 MeV/c is in progress.

## 5.2 Antiproton-deuteron annihilation into $\Lambda K^0$ and $\Sigma^0 K^0$

The study of these so-called Pontecorvo reactions with the production of strange baryons is expected to probe quark dynamics. With stopping antiprotons these reactions can only occur by the interaction of the three incoming nucleons, or by final state rescattering.

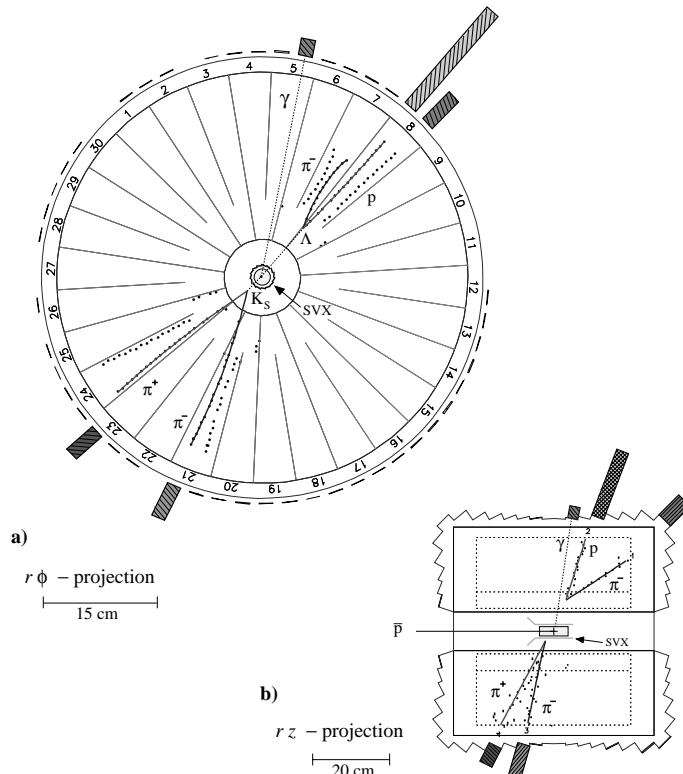


Figure 5.2: A  $\bar{p}d \rightarrow \Sigma^0 K_S$  event ( $K_S \rightarrow \pi^+\pi^-$ ,  $\Sigma^0 \rightarrow \Lambda\gamma$ ) seen by the event display; a) transverse view showing the reconstructed tracks in the jet drift chamber (note the left-right ambiguity of hits in the chamber sectors) and the energy deposits in the barrel; b) view along the beam axis. SVX denotes the silicon microstrip detector.

In two-step processes the  $\bar{p}$  annihilates on the proton producing a  $K^0 \bar{K}^0$  pair. The  $\bar{K}^0$  then interacts with the neutron to generate a  $\Lambda$  or a  $\Sigma^0$ . In contrast, in fireball processes the  $\bar{p}$  interacts simultaneously with the neutron and the proton, generating an ensemble (fireball) of quarks and gluons, which then converts into the observed hadronic final state. For  $\Lambda K^0$  and  $\Sigma^0 K^0$  the two-step mechanism predicts annihilation rates of a few  $10^{-7}$  and  $10^{-9}$ , respectively, while fireball models predict rather similar values in the  $10^{-6}$  range. The ratio of the two branching fractions is considered to be fairly independent of model parameters in both approaches. The large difference of the two-step branching fractions arises from the much larger  $KN\Lambda$  coupling, compared to  $KN\Sigma^0$ . In contrast, the branching ratios for  $\Sigma^0 K^0$  and  $\Lambda K^0$  are equal in the fireball model.

A  $K^0$  and  $\Lambda$  enriched sample of events with antiprotons stopped in a liquid deuterium target was recorded with the Crystal Barrel experiment [9, 10]. This corresponds to about  $10^9$  annihilations. The  $\Lambda$  and  $K^0 \equiv K_S$  have a sufficiently large lifetime to travel several cm before decaying. The silicon microstrip detector surrounding the liquid hydrogen target [11] was therefore used to determine online the charge multiplicity close to the annihilation vertex, while at larger distances the multiplicity was recorded by the jet drift chamber. We studied the final states  $\Lambda K_S$  and  $\Sigma^0 K_S$  with  $\Sigma^0 \rightarrow \Lambda \gamma$ ,  $\Lambda \rightarrow p \pi^-$ ,  $K_S \rightarrow \pi^+ \pi^-$ , and the equivalent final states  $\Lambda K_L$  and  $\Sigma^0 K_L$  (with noninteracting and therefore undetected  $K_L$ ). The trigger recorded data with either one or two secondary vertices, corresponding to a multiplicity increase from 0 to 2 for  $\Lambda K_L$  and  $\Sigma^0 K_L$ , or from 0 to 4 for  $\Lambda K_S$  and  $\Sigma^0 K_S$  events, respectively. These triggers enriched the Pontecorvo channels by roughly two orders of magnitude with respect to a minimum bias experiment. A  $\Sigma^0 K_S$  event is shown in fig. 5.2.

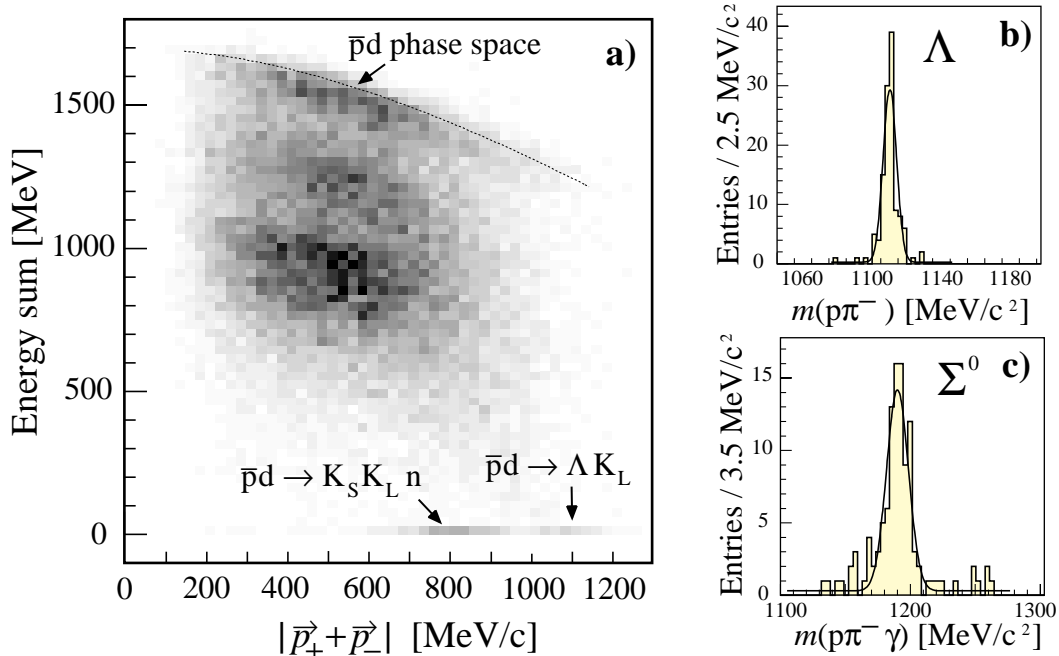


Figure 5.3: a): Total energy measured in the barrel versus total charged particle momentum for the 2-prong sample; b) invariant  $p\pi^-$  mass showing the  $\Lambda$ . The fit (curve) gives a  $\Lambda$  mass of  $1116 \text{ MeV}/c^2$  and an r.m.s resolution of  $4 \text{ MeV}/c^2$ ; c) invariant  $p\pi^-\gamma$  mass for 2-prong events with the  $p\pi^-$  mass consistent with  $\Lambda$  decay and an additional single  $\gamma$ , showing the  $\Sigma^0$ . The fit (curve) gives a  $\Sigma^0$  mass of  $1190 \text{ MeV}/c^2$  and an r.m.s resolution of  $8 \text{ MeV}/c^2$ . The corresponding tabulated values for the  $\Lambda$  and  $\Sigma^0$  masses are  $1115.7$  and  $1192.6 \text{ MeV}/c^2$ .

Samples of about  $10^6$  events each were collected with the 2- and 4-prong topological triggers. The majority of events, of the type  $K^0\bar{K}^0m\pi^0$  ( $m=0,1,2,\dots$ ) with a low energy undetected neutron, could be rejected offline since the detector had an acceptance close to  $4\pi$  for photons. The data samples were cleaned up by requiring unambiguous single or double vertex fits for two or four charged particles with opposite charges. Backscattered charged particles from the CsI barrel were eliminated by a cut requiring an upper limit for the opening angles at the vertices. Entries in the crystal barrel, not matching charged particle trajectories, were identified as photons if the energy deposit in the central crystal amounted to more than 13 MeV. Protons were distinguished from pions through their energy losses in the jet drift chamber. Figure 5.3a shows for instance the total energy measured in the CsI barrel as a function of total momentum carried off by the charged particles in the 2-prong sample. The dominant processes (broad bands bottom to top) stem from  $\Lambda K^0 m\pi^0$  with  $K_L$  missing,  $K_L$  detected and  $K_S \rightarrow \pi^0\pi^0$ . The channel  $\Lambda K_L$  is clearly separated from background. The corresponding plot of barrel energy vs. total momentum carried off by the charged particles and a single photon (channel  $\Sigma^0 K_L$ ) looks similar. Figure 5.3b and c show clear and nearly background free  $\Lambda$  and  $\Sigma^0$  peaks in the  $p\pi^-$  and  $\pi^-p\gamma$  invariant mass spectra after all cuts. Full details on the reconstruction procedure can be found in ref. [10].

We obtained 107  $\Lambda K_L$  and 83  $\Sigma^0 K_L$  events. The corresponding event numbers for  $\Lambda K_S$  and  $\Sigma^0 K_S$  were 85 and 61, respectively. The branching ratios for these reactions are consistent for the 2- and 4-prong samples, giving the average  $(2.35 \pm 0.45) \times 10^{-6}$  for  $\Lambda K^0$  and  $(2.15 \pm 0.45) \times 10^{-6}$  for  $\Sigma K^0$ , in good agreement with predictions from the fireball model [12]. These rates exceed by far the values expected from two-step models. The relative rate is close to unity ( $0.92 \pm 0.15$ ) and agrees with calculations from the fireball model. With the present understanding of meson - baryon interaction, this means that the two-step mechanism is inadequate to describe these Pontecorvo reactions. Our results are consistent with the original nucleonic quarks being dissolved in a large bag with baryon number  $B=1$ .

## References

- [1] P. Giarritta, PhD Thesis, Universität Zürich (2000).
- [2] C. Amsler et al., Phys. Lett. B 311 (1993) 362.
- [3] For a review see C. Amsler, Rev. Mod. Phys. 70 (1998) 1293.
- [4] D. Aston et al., Phys. Lett. B 201 (1988) 573.
- [5] A. Abele et al., Phys. Lett. B 415 (1997) 280.
- [6] M. Heinzelmann, PhD Thesis, Universität Zürich, in preparation.
- [7] C. Amsler, Proc. 8th Int. Conf. on Hadron Spectroscopy, Beijing (1999), Nucl. Phys. A (in print).
- [8] C. Amsler, Proc. Workshop on Hadron Spectroscopy, Frascati Physics Series, Vol. XV (1999) p. 609.
- [9] C. Regenfus, Proc. XVth Particles and Nuclei Int. Conf., Uppsala, 1999 (in print).
- [10] A. Abele et al., Phys. Lett. B 469 (1999) 276.
- [11] C. Regenfus, Nucl. Instr. Meth. in Phys. Res. A 386 (1997) 60.
- [12] J. Cugnon and J. Vandermeulen, Phys. Lett. B146 (1984) 16, Phys. Rev. C39 (1989) 181.